Organic Geochemistry 162 (2021) 104301

Contents lists available at ScienceDirect

Organic Geochemistry

journal homepage: www.elsevier.com/locate/orggeochem

Organic geochemical heterogeneity of the Cretaceous Abu Gabra Formation and reassessment of oil sources in the Sufyan sub-basin, Sudan

Hong Xiao [a,b], Tieguan Wang [a,b], Meijun Li [a,b,*], Dingsheng Cheng [c], Zhe Yang [d]

[a] State Key Laboratory of Petroleum Resources and Prospecting, China University of Petroleum, Beijing 102249, China
[b] College of Geosciences, China University of Petroleum, Beijing 102249, China
[c] Research Institute of Petroleum Exploration and Development, PetroChina, Beijing 100083, China
[d] Exploration and Development Research Institute of PetroChina Jilin Oilfield Company, Songyuan 138000, China

ARTICLE INFO

Associate Editor—**Clifford Walters**

Keywords:
Biomarkers
Source rock evaluation
Source rock heterogeneity
Abu Gabra Formation
Oil sources
Sufyan sub-basin

ABSTRACT

The Lower Cretaceous Abu Gabra Formation (AG) is considered to contain the major source rocks in the Sufyan sub-basin, Sudan. Although prior studies have established the presence of organic-rich lacustrine mudstones, the geochemical heterogeneity of organic facies, thermal maturity, and molecular nature of individual members of the Abu Gabra Formation are insufficiently characterized for oil-source rock correlation. Here, we report on geochemical analysis of 228 cutting samples utilizing Rock-Eval pyrolysis and TOC measurements, from which twenty samples were chosen for investigation of saturated biomarkers. The well cutting samples are from four members (AG_1, AG_1^2, AG_2^2 and AG_3) comprising the Abu Gabra Formation. These analyses were compared to eleven oils produced from the Abu Gabra sandstones to establish member-specific oil-source correlation. The AG_2^2 and AG_3 members have the greatest source potential, containing a higher content of oil-prone organic matter and more favorable maturity than those of the AG_1^2 and AG_1 members. Biomarker data for the AG_2^2 and AG_3 source rocks indicate that deposition occurred under a moderately stratified and somewhat saline water column with a predominance of algal/bacterial input (Type I kerogen). The AG_2^2 and AG_3 source rocks have entered the window of oil generation. In contrast, the AG_1 and AG_1^2 source rocks were possibly deposited in fresh to slightly saline water conditions, have a greater input of terrigenous organic matter input, and are immature to marginally mature. Oil-oil and oil-source rock correlations suggest that the crude oils in the Sufyan sub-basin are genetically homogenous, belong to a single oil family, and are mainly derived from the AG_2^2 and AG_3 source rocks. Contribution from the AG_1 and AG_1^2 source rocks is not apparent from the molecular distributions and is considered to be negligible. The current study provides valuable guidance of source rock evaluation and oil-source rock correlation, which can be a benefit to future petroleum exploration work in the Sufyan sub-basin.

1. Introduction

The Muglad Basin, one of the most important petroleum basins in the Central African Shear Zone (CASZ) (Fig. 1), consists of a set of non-marine clastic Cretaceous to Quaternary strata (Fig. 2) (Fairhead, 1988; Schull, 1988; Genik, 1993). The Sufyan sub-basin, located in the northernmost Muglad Basin, represents a significant hydrocarbon region in the Sudan with an estimated area of 2800 km^2 (Yassin et al., 2017; 2018) (Fig. 1b). Prior petroleum exploration research has mainly concentrated on the central and southern area (Mohamed et al., 2002; Nie et al., 2004; Wen et al., 2007; Makeen et al., 2015a; Wu et al., 2015). Fewer petroleum system studies have been made on the northwest area (Sufyan sub-basin), resulting in slower exploration interest and a delay in discovery (Zhao et al., 2008; Zhang and Qin, 2009; Yassin et al., 2018). Although the Sufyan sub-basin had been recognized as a favorable exploration target (Mohamed et al., 2002; Zhao et al., 2008; Zhang and Qin, 2009), only three wells were drilled in this region before 2007, and only one of them had oil shows (Qiao et al., 2016). The Sufyan sub-basin achieved an exploration breakthrough in 2007, with the Sufyan C-1 well with oil production exceeding 629 bbls per day (Zhang, 2007; Zhang and Qin, 2009).

With the discovery of significant oil reserves, the Sufyan sub-basin has received greater attention and elements of its petroleum system have been studied including sedimentology and reservoir features

* Corresponding author at: 18 Fuxue Road, Changping District, Beijing 102249, China.
E-mail address: meijunli@cup.edu.cn (M. Li).

https://doi.org/10.1016/j.orggeochem.2021.104301
Received 16 May 2021; Received in revised form 16 August 2021; Accepted 17 August 2021
Available online 21 August 2021

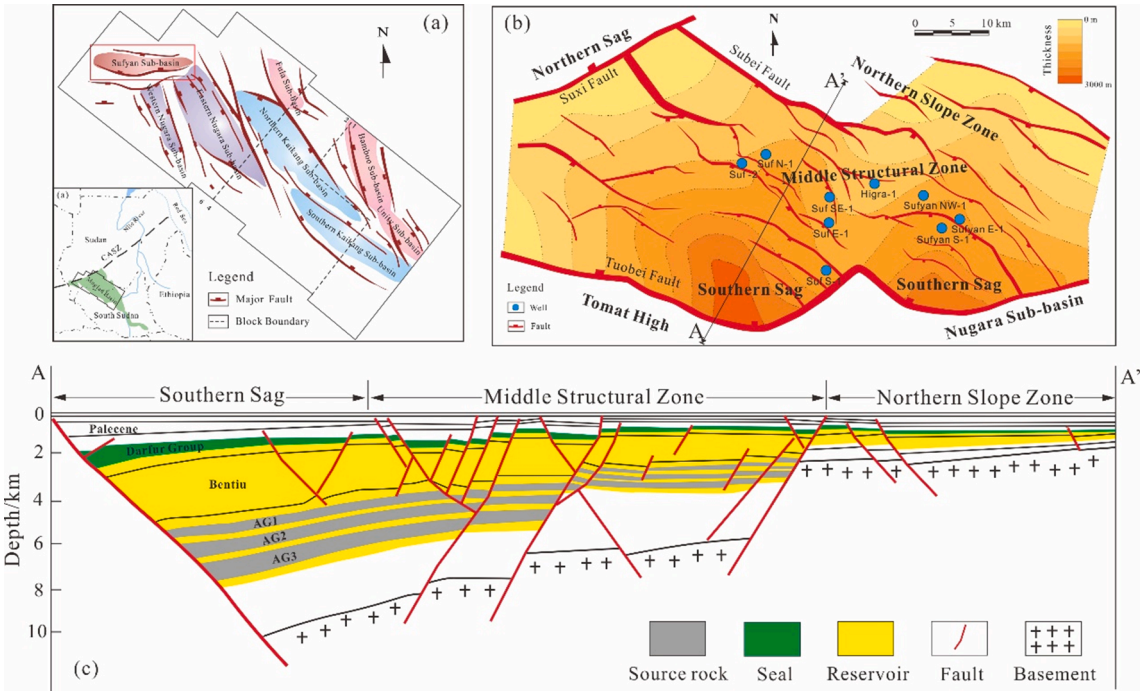

Fig. 1. (a) the location map and structural unit division of the Muglad Basin; (b) structural map of the Sufyan sub-basin and location of wells sampled; (c) Cross-section AA' showing the distribution of the Abu Gabra Formation (modified after Zhang and Qin, 2009; Yassin et al., 2017; Xiao et al., 2019a).

(Genik, 1993; Yassin et al., 2018), tectonic evolution and maturation history modelling (Wang et al., 2016; Yassin et al., 2017), and source rock evaluation and burial history (Zhang, 2007; Zhao et al., 2008; Zhang and Qin, 2009; Qiao et al., 2016). As a promising sub-basin for petroleum exploration, analyses of its hydrocarbon generation potential and oil to source correlations are are required for further exploration work. Dark mudstones in the AG_2 and AG_3 members of the Lower Cretaceous Abu Gabra Formation have high TOC and generative potential containing Type I kerogen (Qiao et al., 2016) and are inferred as the major source of oils produced from sand bodies within the Abu Gabra and the overlying reservoirs in the Bentiu Formation (Zhang and Qin, 2009).

Only a few studies have correlated the Abu Gabra source rocks to associated oils based on molecular geochemistry (Qiao et al., 2016; Xiao et al., 2019d). Their conclusions were based on a limited number of samples from a few wells. In this study, detailed investigation of vertical geochemical heterogeneities within the Abu Gabra Formation source rocks in the Sufyan sub-basin are described. We correlate the vertical heterogeneity of biomarker compositions of these source rocks and determine the relative contribution of individual members to discovered petroleum reservoirs.

2. Geological setting

The Muglad Basin, the largest Mesozoic-Cenozoic petroliferous rift basin in Central African Shear Zone (CASZ), can be further divided into eight sub-basins, including Sufyan, Fula, Unity, Bamboo, North Kaikang, South Kaikang, East Nugara and West Nugara (Schull, 1988; Dou et al., 2013; Xiao et al., 2019a). The Sufyan sub-basin is adjacent to the south of the CASZ and has an east–west trending structural feature (Fig. 1) (Yassin et al., 2017; 2018). It is a half graben-like sub-structural unit with faulting in the south and overlapping in the north (Zhao et al., 2008) (Fig. 1c). The tectonic framework and rifting patterns in the Sufyan sub-basin, as well as hydrocarbon accumulation, were controlled by several major basement faults (Zhang, 2007), including the Suxi, Subei and Tuo faults (Zhang et al., 2009) (Fig. 1). Three rift cycles are present throughout the whole Muglad Basin occurring in the Early Cretaceous, Late Cretaceous and Paleogene (McHargue et al., 1992). Each tectonic cycle is composed of a syn-rift phase and a post-rift phase (thermal sag phase) (Fig. 2) (McHargue et al., 1992).

The sedimentary successions are composed of the Lower Cretaceous Abu Gabra and Bentiu formations, the Upper Cretaceous Darfur Group, the Paleocene Amal, Nayil and Lower Tendi formations, the Neogene Upper Tendi and Adok formations, and the Quaternary Zeraf Formation (Schull, 1988; Xiao et al., 2019a). The thick mudstones of the Abu Gabra Formation are recognized as the main effective hydrocarbon source rock in the entire basin (Qiao et al., 2016). These strata were deposited in a semi-deep to deep lacustrine setting during the first syn-rift phase (Zhao et al., 2008).

Fig. 1 shows that the Southern Sag can be divided into eastern and western parts with separate hydrocarbon generation centers (Zhang and Qin, 2009). The delta sand-body of the Upper Abu Gabra Formation and fluvial channel sand-body of the Bentiu Formation are favorable productive reservoirs, whereas the mudstone interlayers within the Upper Abu Gabra Formation and Darfur Group are significant cap rocks (Fig. 2) (Zhang, 2007). In the study area, most oil and gas accumulation were discovered in fault nose and fault block reservoirs in the Central Structure Belt, which is a tectonic development zone in the Sufyan sub-basin (Zhang, 2007; Zhao et al., 2008). Vertically, the Sufyan sub-basin consists of two petroleum systems (Zhao et al., 2008; Zhang and Qin, 2009). The Abu Gabra Formation, an independent petroleum system, is a self-generating, self-accumulating and self-sealing system. The other is the Abu Gabra Formation-Darfur Group petroleum system consisting of the Abu Gabra Formation source rock, channel sandstone reservoir of the Bentiu Formation and regional seal of the Darfur Group (Zhao et al., 2008; Zhang and Qin, 2009). Thus, the Abu Gabra Formation source rock is the unique and effective source rock in the area (Zhao et al., 2008; Zhang and Qin, 2009; Makeen et al., 2015b; Qiao et al., 2016; Xiao et al., 2019a).

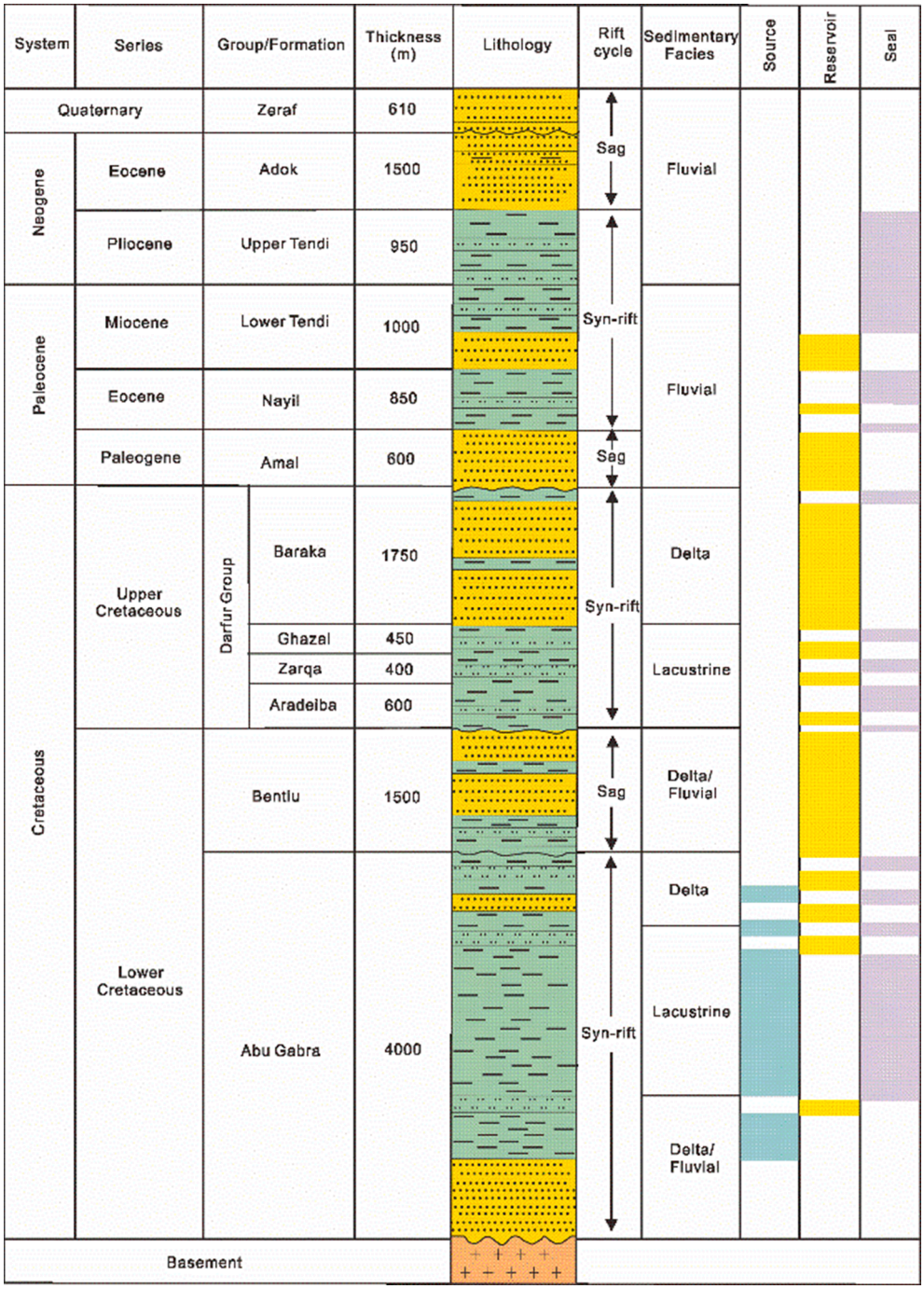

Fig. 2. Generalized stratigraphic column of the Sufyan sub-basin, Muglad Basin (modified after McHargue et al., 1992; Dou et al., 2013; Xiao et al., 2019a).

Table 1
Rock-Eval pyrolysis and TOC data of the Abu Gabra Formation source rocks in the Sufyan sub-basin. Note: RV is range of value; AV is average value.

Sample (mudstone)	S_1 (mg/g)		S_2 (mg/g)		$S_1 + S_2$ (mg/g)		Tmax (°C)		TOC (%)		HI (mg/g)	
	RV	AV	RV	AV	RV	AV	RV	AV	RV	AV	RV	AV
AG1	0.02–0.50	0.10	0.04–14.2	2.36	0.05–14.7	2.46	429–445	438	0.17–2.45	0.94	23.2–80.2	201
AG_1^2	0.06–0.37	0.17	1.97–22.0	8.13	2.06–22.2	8.30	438–447	443	0.62–3.39	1.74	181–722	447
AG_2^2	0.05–0.85	0.26	2.31–59.5	16.64	2.40–59.8	16.9	439–455	447	0.73–6.61	2.66	205–900	583
AG3	0.23–1.05	0.45	8.37–32.7	20.49	8.62–33.2	20.9	443–455	447	1.79–4.10	3.17	455–857	631

3. Analyzed samples and experimental methods

3.1. Source rocks and crude oils

A total of 228 rock cuttings of the Abu Gabra Formation in Sufyan sub-basin were analyzed, of which 20, 35 and 173 are from Sufyan NW-1 well, Higra-1 well and Suf S-1 well, respectively. Twenty mudstone samples were further chosen for systematic biomarker analysis. In addition, eleven crude oil samples from the sandstone reservoirs within the Abu Gabra Formation were geochemically analyzed for biomarker compositions. The sampling well locations are shown in Fig. 1.

3.2. Rock-Eval pyrolysis and total organic carbon (TOC) analyses

The total organic carbon (TOC) content of all potential source rock samples (228 cuttings) was measured using a LECO CS-230 carbon analyzer. Approximately 100 mg of powered sample was crushed to 80 mesh, treated with diluted HCl to remove inorganic carbon, washed with deionized water for two days to remove remaining contaminants, and finally dried in an oven at 80 °C for one day. Rock-Eval parameters of 228 rock cuttings (Table 1) were measured using an initial temperature of 300 °C held for 3 min, then heating at 25 °C/min up to 600 °C.

3.3. Extraction and separation processes

The extractable organic matter (EOM) of twenty mudstone samples was obtained from about 100 g of powdered samples using a Soxhlet apparatus with 400 mL of dichloromethane/methanol (93:7, v/v) for 48 h. Solvent-extracted hydrocarbons and crude oils were dissolved in 50 mL of petroleum ether, and then filtered through a funnel stuffed with a little clean cotton to remove insoluble compounds (asphaltenes). The residual solutions were separated into saturated hydrocarbon, aromatic hydrocarbon and resin fractions using a silica gel/alumina standard chromatography column with sequential addition of petroleum ether, mixed reagent of dichloromethane and petroleum ether (2:1, v/v), and mixed reagent of dichloromethane and methanol (93:7, v/v), respectively.

3.4. Gas chromatography–mass spectrometry

Molecular analysis of the saturated hydrocarbon fractions of selected rock extracts and crude oils were conducted using an Agilent 6890 gas chromatograph coupled to an Agilent 5975i mass selective detector. Separation was achieved using an HP-5 MS fused silica capillary column (60 m × 0.25 mm i.d., 0.25 μm film coating) with helium as the carrier gas. Upon injection at 300 °C, the GC initial oven temperature of 50 °C was increased at a rate of 20 °C/min to 120 °C, then to a final temperature of 310 °C at 3 °C/min. The MS was operated with electron impact ionization at 70 eV with a full scan range of 50–600 Da.

4. Results and discussion

4.1. Evaluation of the Abu Gabra source rocks

4.1.1. Hydrocarbon generation potential

In the study, 228 cutting samples from the Abu Gabra Formation were analyzed to determine the abundance, type and maturity of the organic matter. The Abu Gabra Formation is usually divided into three members (AG_1, AG_2 and AG_3) (Luo et al., 1998; Xu et al., 2003; Qiao et al., 2016). According to the detailed stratigraphic classification data provided from the China National Petroleum Corporation, the AG_2 member can be further sub-divided into five beds (AG_{2a}, AG_{2b}, AG_{2c}, AG_{2d} and AG_{2e}) on the basis of the lithologic composition and sedimentary environment. The AG_{2a} is represented by AG_1^2, while the AG_{2b}–AG_{2e} are uniformly classified as AG_2^2 in this study.

Hunt (1996) proposed that the plot of S_1 (mg HC/g rock) versus TOC (%) can effectively discriminate an indigenous and non-indigenous hydrocarbon in source rock samples (Hunt, 1996). Generally, a value of S_1/TOC > 1.5 indicates that the source rocks are distinctly contaminated with migrated hydrocarbon (Mashhadi and Rabbani, 2015). In the study, S_1/TOC values of all cutting samples are < 1.5, which indicates an indigenous nature for associated hydrocarbon (Fig. 3). Moreover, the AG_1 and AG_1^2 mudstone samples present an apparently lower organic matter abundance (TOC and S_1) than that of the AG_2^2 and AG_3 mudstones samples (Fig. 3).

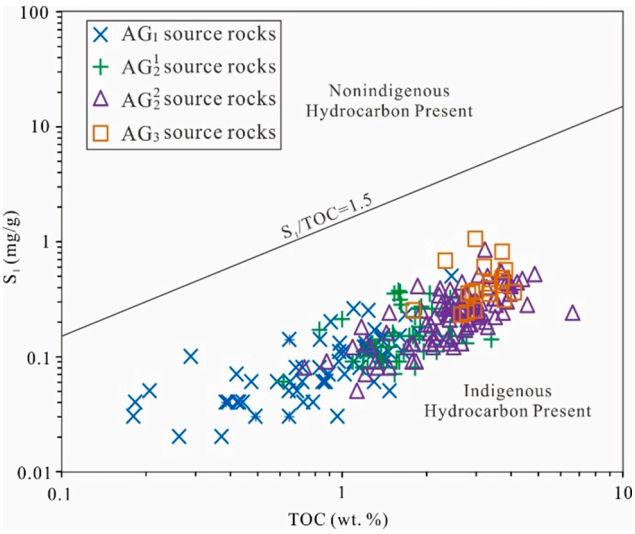

Fig. 3. Plot of S_1 vs TOC to distinguish between indigenous and non-indigenous hydrocarbons in the rock cuttings (Hunt, 1996).

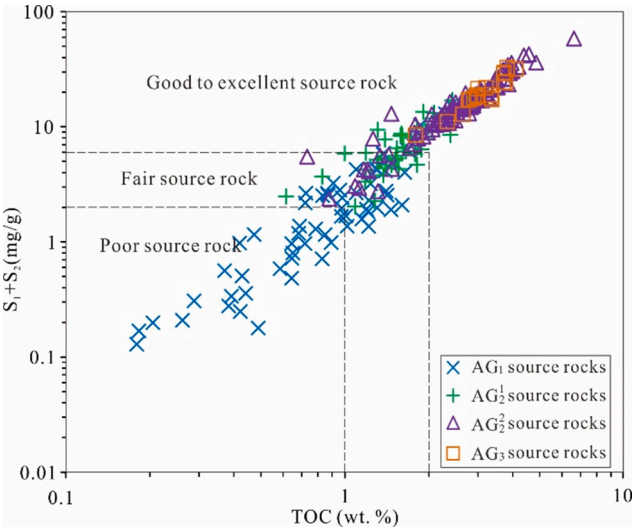

Fig. 4. Plot of $S_1 + S_2$ vs TOC indicating the quality of the Abu Gabra source rocks in the Sufyan sub-basin.

The TOC content (wt%) and hydrocarbon generation potential ($S_1 + S_2$, mg HC/g rock) of the mudstones exhibit a wide range of values, from 0.17% to 6.61% and 0.05 mg/g to 59.8 mg/g, respectively. In Fig. 4a ($S_1 + S_2$ vs TOC) (Liu et al., 2017; Xiao et al., 2019d), the mudstone samples from the Abu Gabra Formation (AG_1, AG_1^2, AG_2^2 and AG_3) show an obviously heterogeneous distribution. The hydrocarbon generation potential of the most of the AG_2^2, AG_3 and some of the AG_1^2 mudstone samples are >6.0 mg HC/g rock, falling into the region of good-to-excellent source rocks (Fig. 4a). Whereas the AG_1 and other AG_1^2 mudstone samples are mostly distributed in the area of rocks having only poor-to-fair generation potential with a $S_1 + S_2$ values

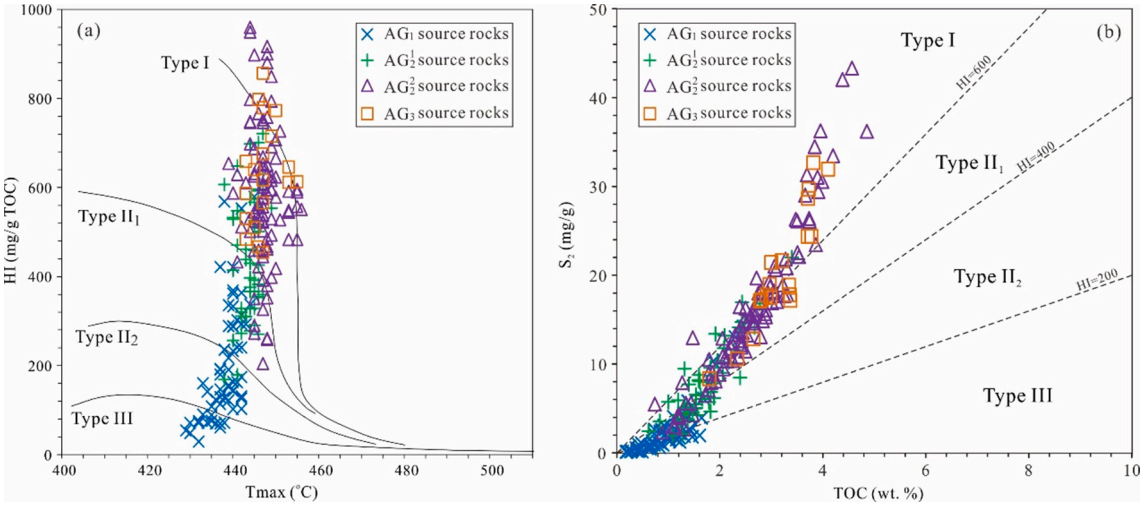

Fig. 5. (a) Variation of hydrogen index with Tmax of the Abu Gabra Formation source rocks showing the organic matter type; (b) plot of S_2 vs TOC showing kerogen type of the Abu Gabra Formation source rocks.

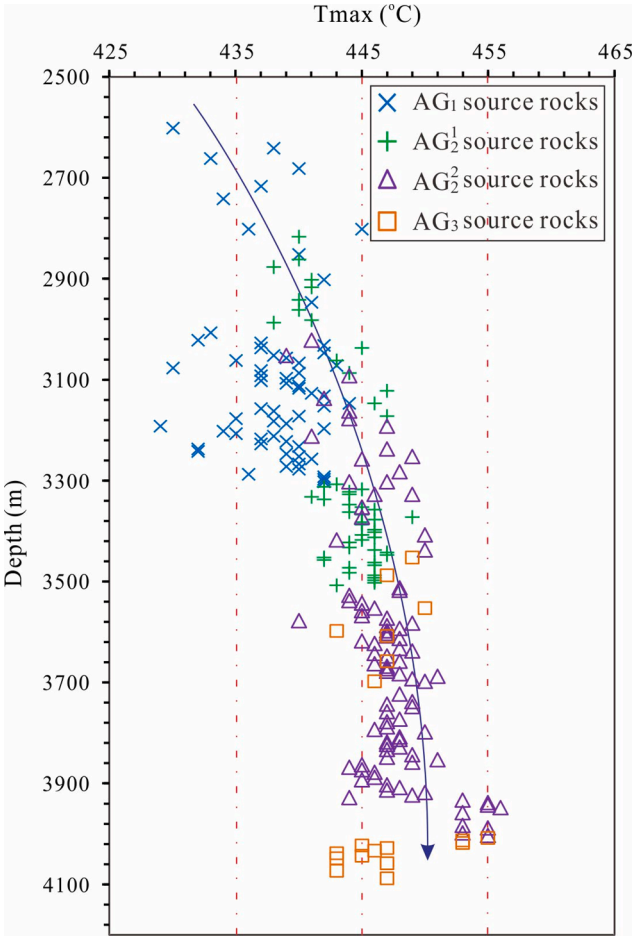

Fig. 6. Variations of Tmax (°C) values of the AG samples with increasing burial depth.

ranging from 0.1 mg HC/g rock to 6.0 mg HC/g rock. A few of the AG_1 samples are below the minimal standard to be considered effective source rock (Table 1). Hydrocarbon index (HI) values of the AG_1, AG_1^2, AG_2^2 and AG_3 mudstone samples are in the ranges of 23.2–581 (mean = 200 mg HC/g rock), 180–722 (mean = 447 mg HC/g rock), 205–900 (mean = 583 mg HC/g rock), and 455–858 (mean = 631 mg HC/g rock), respectively (Table 1).

4.1.2. Type of organic matter

The organic matter type of the AG_1, AG_1^2, AG_2^2 and AG_3 mudstones was characterized by %TOC and Rock-Eval parameters (HI, S_2 and Tmax). Generally, type I–II_1 kerogens commonly have HI values >300 mg HC/g TOC. Plot of HI vs Tmax (Mukhopadhyay et al., 1995; Hao et al., 2007; Liu et al., 2017; Lai et al., 2019; Xiao et al., 2019d) show than most of the AG_1 and some of the AG_1^2 mudstone samples are distributed in the zone of type II_2–III kerogen (Fig. 5a), consistent with mixed organic matter sources of aquatic and terrigenous organic matter input deposited under oxic or sub-oxic waters. The AG_2^2, AG_3 and other AG_1^2 mudstone samples generally plot in the type I–II_1 kerogen zone possibly indicating a predominant contribution of algal and/or bacterial input (Fig. 5a).

The kerogen type of the AG_1, AG_1^2, AG_2^2 and AG_3 mudstones can be further classified by hydrocarbon pyrolysis yields (S_2) and %TOC values (Makeen et al., 2015b). As shown in Fig. 5b, the AG_2^2 and AG_3 samples mostly plot in the field for type I–II_1 kerogen with high S_2 and TOC values, whereas the AG_1 and AG_1^2 mudstone samples contain relative low values of S_2 and %TOC (Table 1) that are characteristic of II_2–III kerogen (Fig. 5b).

4.1.3. Maturity of organic matter

The temperature at maximum pyrolysis yield (Tmax, °C) is commonly used as a screening measurement of source rock thermal maturity. Tmax values of the Abu Gabra Formation samples show a positive relationship with buried depth, which indicates that the buried depth acts a primarily controlling factor for thermal maturity (Fig. 6). In the Sufyan NW-1, Higra-1 and Suf S-1 wells, Tmax values of the AG_1^2, AG_2^2 and AG_3 mudstone samples are in the range of 438–447 °C, 439–455 °C and 443–455 °C respectively (Table 1), corresponding to the main oil generation window (Fig. 6). The maturity of the AG_1 mudstone samples exhibit the lowest values and several of the AG_1 samples are still in the immature stage (Tmax < 435 °C) (Fig. 6 and Table 1).

To summarize, the AG_2^2 and AG_3 mudstones are organically rich Cretaceous source rock candidates in the Sufyan sub-basin. These members have higher hydrocarbon generation potential, better organic matter type and more favorable thermal maturity than the AG_1^2 mudstones. The AG_1 member possesses poor-to-fair hydrocarbon potential and is thermally immature in the analyzed well.

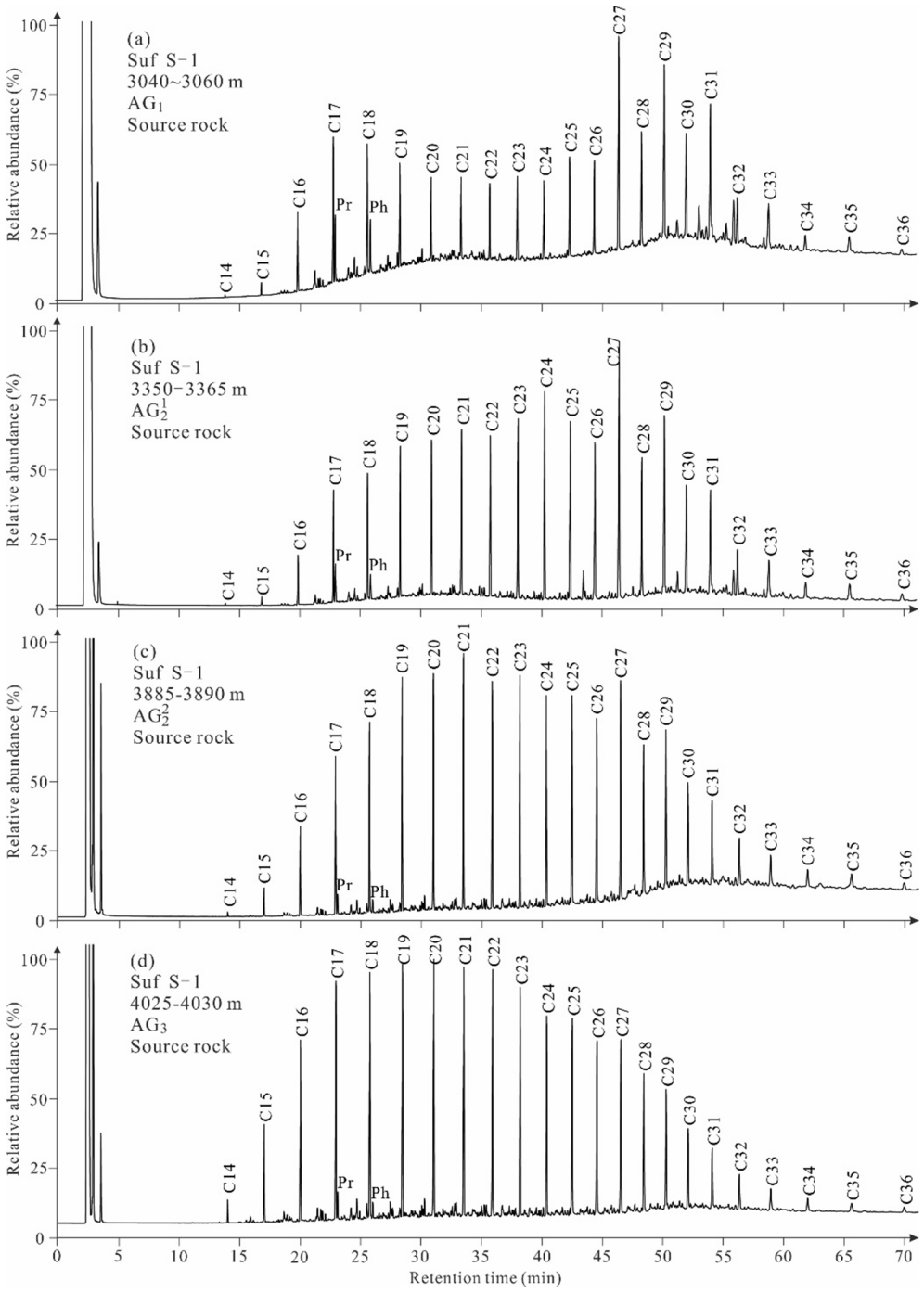

Fig. 7. Representative gas chromatograms of saturated hydrocarbon in the AG_1, AG_1^2, AG_2^2 and AG_3 source rocks from the Sufyan sub-basin.

4.2. Biomarker composition in the Abu Gabra source rocks

4.2.1. n-Alkanes and isoprenoids distributions

In order to clearly show the vertical heterogeneity of the Abu Gabra source rocks, four rock extracts from the same well (Suf S-1 well) at different depths were selected to illustrate their variation in organic matter content, composition and depositional conditions. All samples have a full *n*-alkane series ranging from *n*-C_{14} to *n*-C_{36}, and their relative abundances are much higher than that of isoprenoids (Fig. 7). Pr/Ph ratios vary from 1.02 to 1.95 (Table 2), indicating that oxic to sub-oxic depositional conditions prevailed during deposition of the Abu Gabra Formation. The *n*-alkane series in the AG_1 sample displays a bimodal pattern with a strong odd-carbon number preference from *n*-C_{27}, the main peak, to *n*-C_{31} (Fig. 7). These features diminish with depth resulting in a unimodal distribution with only a weak *n*-C_{27}–*n*-C_{31} odd-carbon number preference in the AG_3 sample (Fig. 7). Consistent with the Rock-Eval pyrolysis and TOC results, the odd-carbon number preference in the AG_1 and AG_1^2 source rocks is an integrated reflection of greater terrigenous high plant input and low thermal maturation (Bray and Evans, 1961; Scalan and Smith, 1970; Peters et al., 2005; Zhu and Jin, 2008).

4.2.2. Tricyclic terpanes distribution

Tricyclic terpanes (TTs) is extensively distributed in source rocks that are deposited in a variety of sedimentary environments (Ekweozor and Strausz, 1983; Xiao et al., 2018, 2019c). The marine or saline lacustrine

Table 2
Molecular parameters composition for the Abu Gabra Formation source rocks from the Sufyan sub-basin.

Nom.	Well name	Depth/m	Member	Samples	Pr/Ph	$C_{19+20}TT$ %	$C_{21}TT$ %	$C_{23}TT$ %	Ga/$C_{30}H$	$C_{30}D$/$C_{30}H$	$C_{30}E$/$C_{30}H$	$C_{27}D$/$C_{27}St$	C_{27}/$C_{29}St$	C_{29} 20S/(20S + 20R)
1	SufyanNW-1	2800–2805	AG_1	cutting	1.15	34.3	33.8	31.8	0.04	0.03	0.04	0.28	0.75	0.27
2		3060–3090	AG_1^2	cutting	1.15	41.9	32.2	25.9	0.05	0.08	0.14	0.51	1.08	0.38
3		3190–3255	AG_1^2	cutting	1.48	39.7	33.5	26.8	0.15	0.09	0.15	0.47	1.16	0.35
4		3435–3440	AG_2^2	cutting	1.88	45.2	32.8	22.1	0.19	0.14	0.18	0.60	1.18	0.42
5	Higra-1	2715–2745	AG_1	cutting	1.08	38.0	36.9	25.1	0.08	0.05	0.06	0.33	0.88	0.23
6		2900–2905	AG_1^2	cutting	1.95	46.0	30.2	23.8	0.05	0.08	0.17	0.45	1.27	0.26
7		3090–3095	AG_2^2	cutting	1.89	39.0	37.6	23.5	0.21	0.10	0.15	0.48	1.21	0.30
8		3255–3260	AG_2^2	cutting	1.85	41.8	36.0	22.2	0.20	0.15	0.16	0.60	1.23	0.49
9		3655–3660	AG_3	cutting	1.55	47.5	33.5	19.0	0.25	0.32	0.33	0.86	1.04	0.55
10	Suf S-1	3040–3060	AG_1	cutting	1.10	31.1	38.5	30.5	0.03	0.04	0.06	0.22	0.44	0.26
11		3170–3180	AG_1	cutting	1.51	35.0	40.1	24.9	0.04	0.06	0.07	0.37	0.55	0.22
12		3265–3275	AG_1	cutting	1.02	31.5	41.2	27.3	0.07	0.05	0.05	0.40	0.67	0.28
13		3350–3365	AG_1^2	cutting	1.44	33.6	40.9	25.5	0.07	0.07	0.10	0.51	0.94	0.32
14		3440–3445	AG_1^2	cutting	1.73	40.2	40.1	19.7	0.10	0.08	0.07	0.48	1.00	0.36
15		3570–3585	AG_2^2	cutting	1.44	38.6	37.2	24.2	0.26	0.22	0.23	0.85	1.40	0.50
16		3655–3660	AG_2^2	cutting	1.46	39.9	38.4	21.8	0.27	0.22	0.21	0.82	1.32	0.53
17		3720–3725	AG_2^2	cutting	1.67	41.1	36.2	22.7	0.33	0.29	0.29	0.78	1.15	0.63
18		3885–3890	AG_2^2	cutting	1.23	40.3	34.9	24.7	0.32	0.29	0.27	0.76	1.19	0.51
19		3995–4000	AG_2^2	cutting	1.41	38.2	36.1	25.7	0.22	0.31	0.27	0.59	1.06	0.55
20		4025–4030	AG_3	cutting	1.61	41.1	36.1	22.7	0.30	0.37	0.37	0.75	1.10	0.62

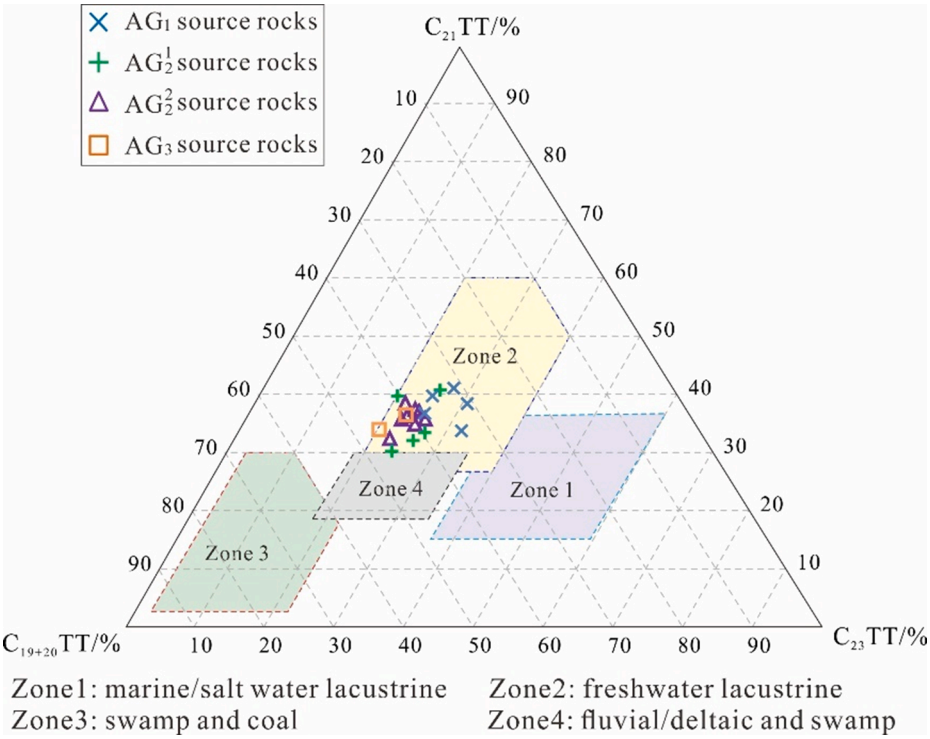

Fig. 8. A ternary diagram of $C_{19+20}TT$, $C_{21}TT$ and $C_{23}TT$ to discriminate the various depositional environments (after Xiao et al., 2019c).

source rocks and their related oils are usually dominated by $C_{23}TT$ among C_{19}–$C_{23}TT$ homologues (Aquino Neto et al., 1983; Chen et al., 2017), whereas coal samples usually contain high abundance of $C_{19}TT$ (Zhu, 1997; Fu et al., 2019). Recently, Xiao et al. (2019c) proposed a ternary diagram that distinguishes the depositional environments of the source rocks and related oils based on the analyses of C_{19}–C_{23} TTs of 104 source rocks and 113 oils from several different basins (Xiao et al., 2019c). In general, $C_{19}TT$ and $C_{20}TT$ are more abundant in swamp source rocks with terrigenous organic matter input, while sediments deposited in freshwater lacustrine are characterized by a dominance of $C_{21}TT$ (Xiao et al., 2019c). Fig. 8 illustrates that the Abu Gabra source rocks have a consistent distribution pattern of C_{19}–$C_{23}TT$, with $C_{21}TT$ as a dominant homologue, indicating a freshwater lacustrine depositional setting.

4.2.3. Hopane distributions

Gammacerane is a diagnostic biomarker for water column stratification (Hills et al., 1966; Moldowan et al., 1985; Sinninghe Damsté et al., 1995). The origin of gammacerane is uncertain, but it is possibly derived from a reduction product of tetrahymanol during diagenesis (Venkatesan and Dahl, 1989). Tetrahymanol is synthesized by a variety of bacteria (aerobic methanotrophs, nitrate-oxidizers and sulfate reducers, and by a subset of aquatic (ciliates) and terrestrial eukaryotes (Banta et al., 2015). Fig. 9 shows that the AG_2^2 and AG_3 source rocks have a significant abundance of gammacerane, greater than C_{31} hopanes, indicating moderate salinity depositional condition. However,

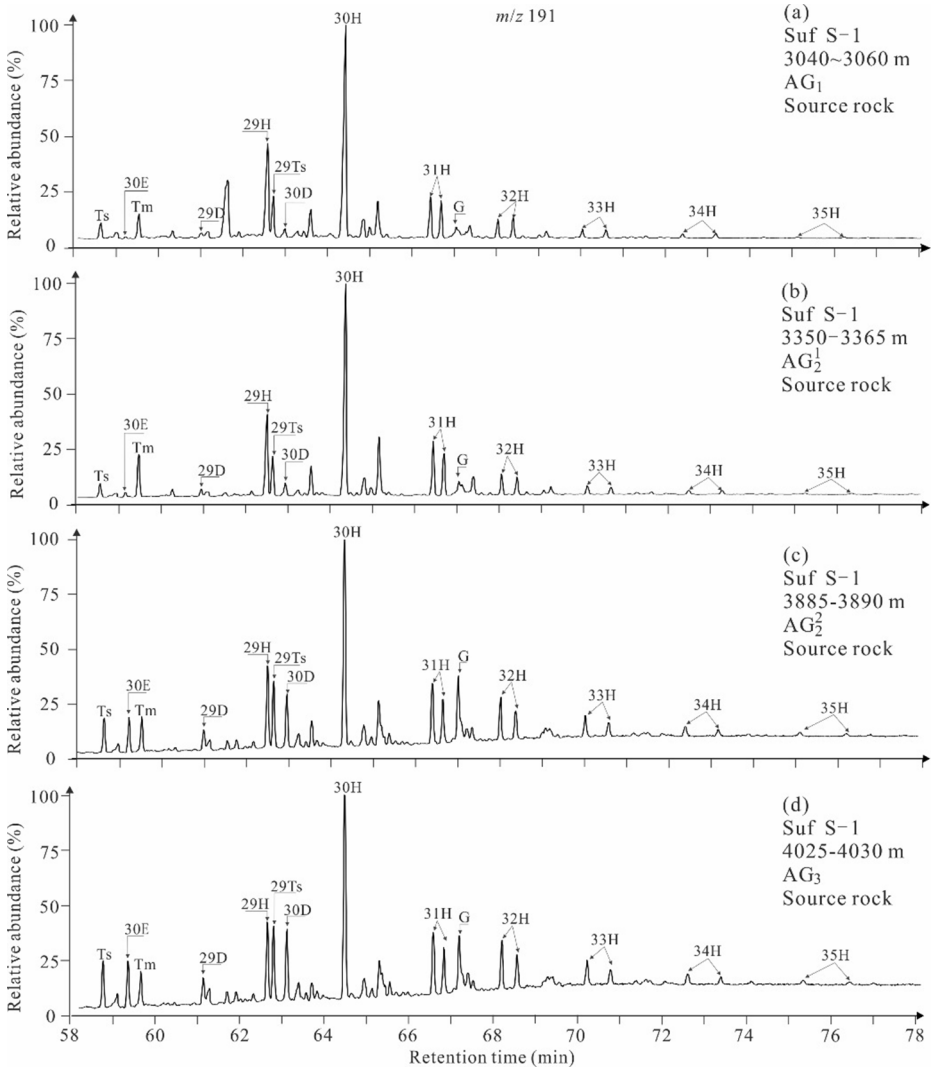

Fig. 9. Distributions of hopanes and gammacerane (*m/z* 191) in mudstone extracts from the AG_1, AG_1^2 AG_2^2 and AG_3 source rocks in the Sufyan sub-basin.

its abundance in the AG_1 and AG_1^2 source rocks is extremely low and almost at the detection limit in a few samples, which is commonly associated with a freshwater lacustrine depositional setting.

Moldowan et al. (1991) proposed that the rearranged hopane series is derived from bacteriohopanoid precursors by a catalysis of acidic clay minerals under oxic or sub-oxic conditions (Moldowan et al., 1991). In the study, the rearranged hopanes distribution in the upper (AG_1 and AG_1^2) and lower (AG_2^2 and AG_3) members are significantly different. Specifically, the AG_2^2 and AG_3 source rocks contain high abundance of 17α(H)-diahopanes (D) and early eluting series (E), whereas those in the AG_1 and AG_1^2 source rocks are in very low abundance or completely absent (Fig. 9). This result demonstrates that there are major differences in the organic matter composition and/or sedimentary environment between the upper and lower members of the Abu Gabra Formation.

The C_{31}–C_{35} hopanes (homohopane series) distribution is useful to assess redox conditions and oil-source rock correlation (Peters et al., 2005). Generally, a relatively high abundance of C_{35} hopane is attributed to a highly reducing marine or high salinity lacustrine conditions (Peters and Moldowan, 1991; Hao et al., 2011). The distribution pattern of homohopane series in all Abu Gabra source rocks is characterized by a gradual decrease from C_{31} to C_{35} hopanes (Fig. 9), which further implies a fresh to moderate salinity lacustrine sedimentary environment.

4.2.4. *Sterane distributions*

The upper and lower Abu Gabra Formation source facies can be distinguished by regular steranes, diasteranes and 4α-methylsteranes. The upper member source rock contains low concentrations of C_{27} diasteranes, C_{27} regular steranes and C_{30} 4α-methylsteranes (Fig. 10a and b). The lower member source rock is characterized by relatively high abundances of C_{27} diasteranes, C_{27} regular steranes and C_{30} 4α-methylsteranes (Fig. 10c and d). The sterane series is commonly applied to analyze organic matter input and depositional conditions (Huang and Meinschein, 1979; Summons et al., 1987). High C_{27} diasteranes content is usually associated with clay-rich source rocks deposited under oxic or sub-oxic conditions (Peters et al., 2005). The distribution pattern of C_{27}–C_{29} steranes can distinguish oil groups or different organic facies. Generally, a predominance of C_{29} steranes indicates higher-plant input (Peters et al., 2005) or green algae (Summons and Douglas, 2018), whereas C_{27} steranes are a signature of eukaryotic algae (Peters et al., 2005) and animal phyla (Summons and Douglas, 2018). The C_{30} 4α-methylsteranes are mainly derived from freshwater lacustrine algae (Summons et al., 1987; 1992). The comparative analysis indicates that the AG_2^2 and AG_3 source rocks are composed of mixed organic matter input dominated by eukaryotic algae and/or bacteria, while the AG_1 and AG_1^2 source rocks possibly received a greater input of higher plant material.

The 20S/(20S + 20R) and ββ/(ββ + αα) ratios of C_{27}–C_{29} regular

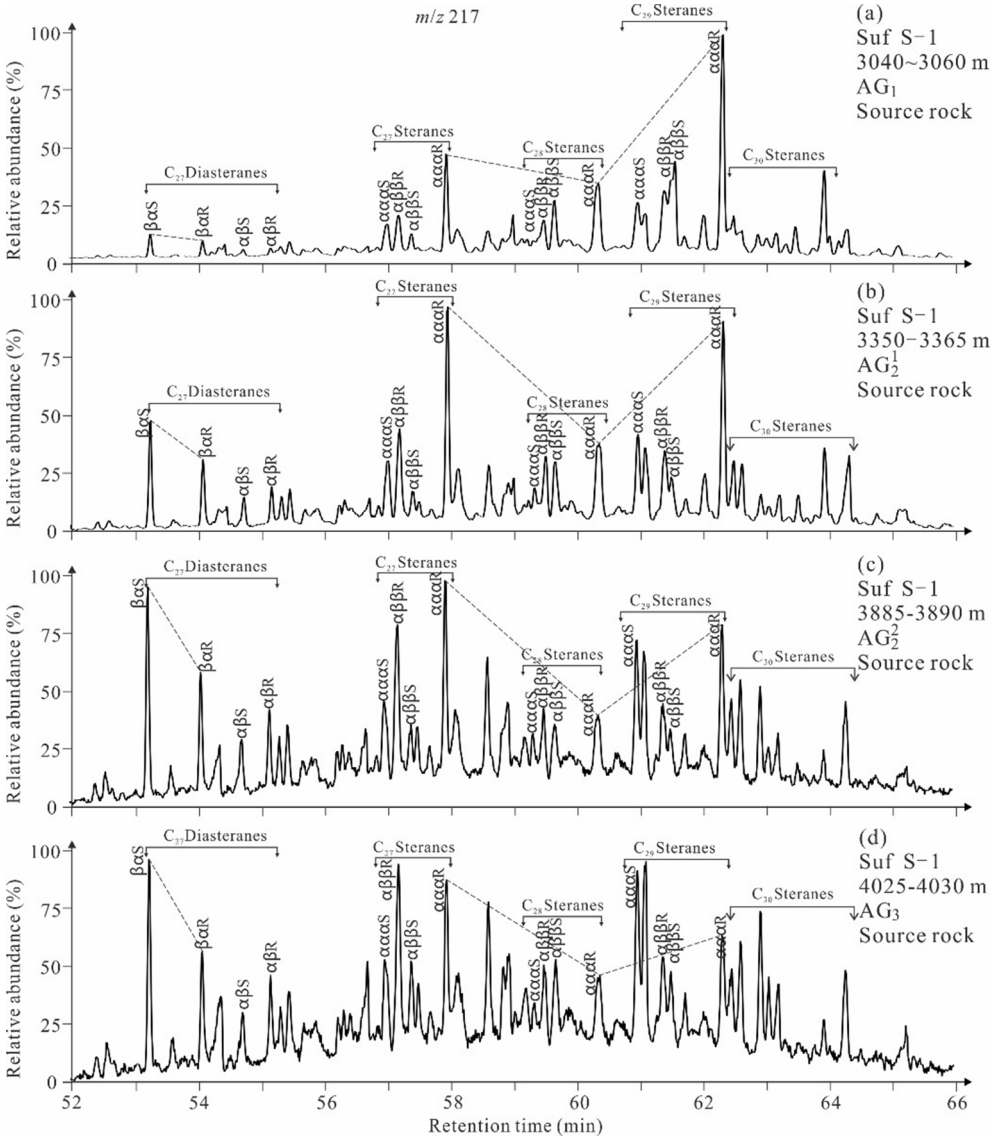

Fig. 10. The distribution of C_{27} diasteranes, C_{27}–C_{29} regular steranes and C_{30} 4α-methylsterane (*m/z* 217) in mudstone extracts from the AG_1, AG_1^2, AG_2^2 and AG_3 source rocks in the Sufyan sub-basin.

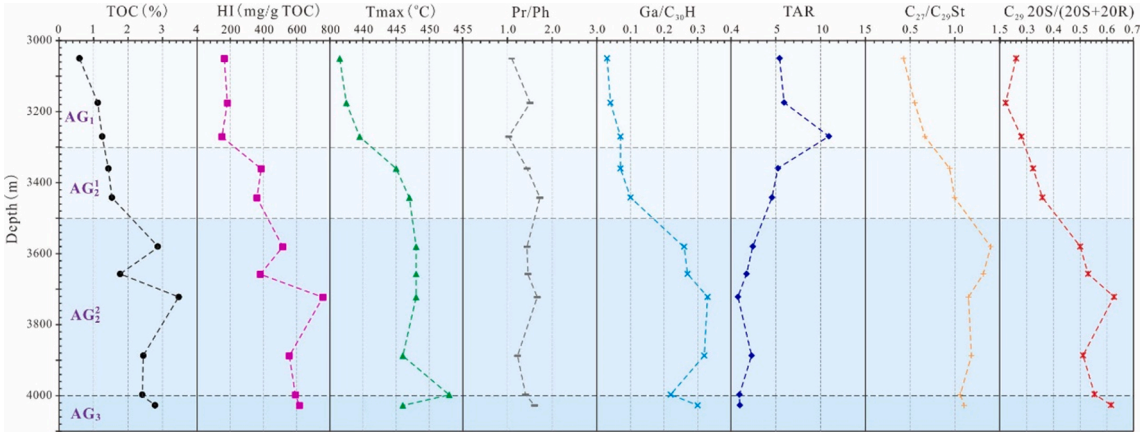

Fig. 11. Vertical variation in organic matter abundance, type, maturity and depositional environment of the Abu Gabra Formation source rocks in the Suf S-1 well.

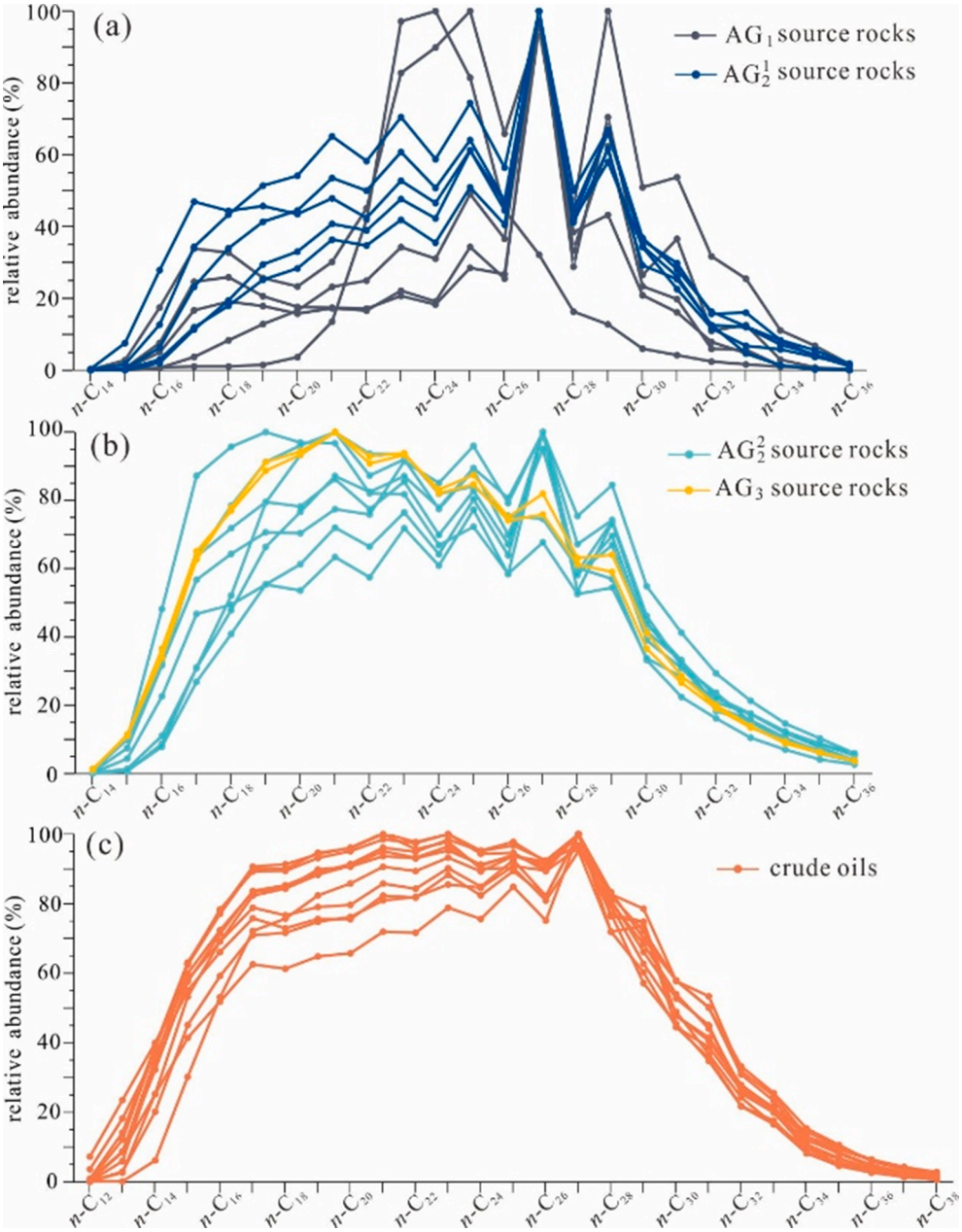

Fig. 12. Line charts of relative abundance of C_{14}–C_{36} (C_{12}–C_{38}) *n*-alkanes in the AG_1, AG_1^2, AG_2^2 and AG_3 source rocks and crude oils indicating different organic matter inputs and thermal maturation.

steranes are effective maturity parameters, in which the 20R and αα are the biological configuration, while the 20S and ββ are the geological configuration (Seifert and Moldowan, 1981; Mackenzie et al., 1982). The 20S/(20S + 20R) and ββ/(ββ + αα) ratios will rise from near-zero values up to 0.5 (0.52–0.55 = equilibrium) and ~ 0.7 (0.67–0.71 = equilibrium) respectively with increasing thermal maturity (Seifert and Moldowan, 1986). The relative abundance of 20S and ββ stereochemistry of C_{27}–C_{29} steranes in the AG_2^2 and AG_3 source rocks are higher than that of the AG_1 and AG_1^2 source rocks corresponding to a higher thermal maturity for the AG_2^2 and AG_3 source rocks (Fig. 10).

4.2.5. Comprehensive comparative analysis

The above discussion addresses the geochemical characteristics including abundance, type and thermal maturity of organic matter, as well as biomarker compositions in the entire Abu Gabra Formation and presents evident vertical heterogeneity. A comprehensive analysis of organic facies reveals that the upper AG_1 and AG_1^2 source rocks are similar and distinct from the lower AG_2^2 and AG_3 members (Fig. 11).

Generally, the AG_2^2 and AG_3 source rocks have a high organic matter abundance (TOC > 2.0% and HI > 400 mg/g rock) corresponding to type I-II_1 kerogen, while the AG_1 and AG_1^2 source rocks contain relative low values of TOC (<2.0%) and HI (400 mg/g rock) with predominantly II_2-III kerogen. According to the maturity-related parameters of Tmax and C_{29} steranes 20S/(20S + 20R), the AG_2^2 and AG_3 source rocks have already entered the main hydrocarbon generation window, but the AG_1 and partial AG_1^2 source rocks are still at the immature to low mature stage (Fig. 11).

All samples from the Abu Gabra Formation show similar Pr/Ph values with the range of 1.0–2.0 indicating oxic to sub-oxic water column conditions. There is a high abundance gammacerane in the AG_2^2 and AG_3 source rocks ($Ga/C_{30}H > 0.25$), and very low abundance or completely absent in the AG_1 and AG_1^2 source rocks ($Ga/C_{30}H < 0.1$)

Table 3
Selected parameters for oil to source rock correlation in the Sufyan sub-basin.

Nom.	Well Name	Depth/m	Formation	Samples	n-C_{21}-/n-C_{21}+	(n-C_{21} + n-C_{22})/(n-C_{28} + n-C_{29})	CPI	OEP	TAR	Pr/n-C_{17}	Ph/n-C_{18}	Pr/Ph	C_{27}%	C_{28}%	C_{29}%	Ga/C_{30}H	C_{30}D/C_{30}H	C_{27}Dia/C_{27}St
1	SufyanNW-1	2800–2805	AG_1	cutting	0.05	0.35	0.78	1.19	3.05	0.31	0.33	1.15	30.6	28.4	40.9	0.04	0.03	0.28
2		3060–3090	AG_1^2	cutting	0.36	0.93	1.37	1.20	2.96	0.23	0.17	1.15	35.7	31.1	33.2	0.05	0.08	0.51
3		3190–3255	AG_1^2	cutting	0.41	1.05	1.27	1.20	2.23	0.15	0.11	1.48	39.7	26.1	34.2	0.15	0.09	0.47
4		3435–3440	AG_2^2	cutting	0.56	1.23	1.16	1.16	1.37	0.13	0.07	1.88	41.8	22.9	35.3	0.19	0.14	0.60
5	Higra-1	2715–2745	AG_1	cutting	0.27	0.85	1.16	1.16	2.48	0.15	0.15	1.08	34.9	25.6	39.5	0.08	0.05	0.33
6		2900–2905	AG_1^2	cutting	0.49	0.90	1.37	1.20	1.80	0.13	0.08	1.95	39.9	28.8	31.3	0.05	0.08	0.45
7		3090–3095	AG_2^2	cutting	0.43	0.95	1.24	1.21	1.94	0.14	0.08	1.89	41.9	23.5	34.6	0.21	0.10	0.48
8		3255–3260	AG_2^2	cutting	0.48	1.08	1.04	1.12	1.50	0.10	0.05	1.85	41.6	24.5	33.9	0.20	0.15	0.60
9		3655–3660	AG_3	cutting	0.62	1.50	0.96	1.07	1.06	0.07	0.04	1.55	38.4	24.8	36.8	0.25	0.32	0.86
10	Suf S-1	3040–3060	AG_1	cutting	0.21	0.24	1.70	1.20	5.43	0.39	0.41	1.10	22.9	24.6	52.5	0.03	0.04	0.22
11		3170–3180	AG_1	cutting	0.23	0.34	2.26	1.29	5.92	0.45	0.32	1.51	27.3	23.1	49.6	0.04	0.06	0.37
12		3265–3275	AG_1	cutting	0.15	0.50	1.81	1.24	10.94	0.49	0.35	1.02	29.6	25.9	44.5	0.07	0.05	0.40
13		3350–3365	AG_1^2	cutting	0.23	0.66	1.51	1.20	5.24	0.28	0.16	1.44	36.1	25.5	38.3	0.07	0.07	0.51
14		3440–3445	AG_1^2	cutting	0.26	0.78	1.48	1.19	4.57	0.25	0.11	1.73	38.4	23.1	38.5	0.10	0.08	0.48
15		3570–3585	AG_2^2	cutting	0.37	1.08	1.17	1.17	2.44	0.16	0.09	1.44	45.9	21.4	32.7	0.26	0.22	0.85
16		3655–3660	AG_2^2	cutting	0.48	1.49	1.10	1.12	1.73	0.14	0.07	1.46	43.4	23.7	32.9	0.27	0.22	0.82
17		3720–3725	AG_2^2	cutting	0.81	1.67	1.00	1.11	0.76	0.13	0.09	1.67	40.3	24.7	35.0	0.33	0.29	0.78
18		3885–3890	AG_2^2	cutting	0.38	1.06	1.03	1.09	2.29	0.10	0.06	1.23	40.9	24.9	34.2	0.32	0.29	0.76
19		3995–4000	AG_2^2	cutting	0.66	1.65	0.92	1.06	0.93	0.05	0.04	1.41	37.8	26.4	35.7	0.22	0.31	0.59
20		4025–4030	AG_3	cutting	0.64	1.61	0.94	1.07	0.98	0.06	0.04	1.61	39.1	25.6	35.4	0.30	0.37	0.75
21	Suf-2	3374–3376	AG_2^2	oil	0.67	1.22	1.08	1.03	0.94	0.17	0.10	1.56	46.5	21.5	32.0	0.26	0.37	0.88
22	Suf E-1	3595–3599	AG_2^2	oil	0.55	1.17	1.10	1.04	1.20	0.18	0.11	1.53	49.2	20.7	30.1	0.31	0.33	0.87
23	Suf N-1	2849–2852	AG_1^2	oil	0.81	1.48	1.14	1.05	0.77	0.19	0.11	1.67	45.7	22.1	32.2	0.27	0.19	0.53
24	Suf SE-1	3185–3187	AG_1^2	oil	0.77	1.39	1.07	1.03	0.79	0.15	0.10	1.49	47.4	22.2	30.4	0.28	0.35	0.80
25		3149–3152	AG_1^2	oil	0.76	1.46	1.08	1.03	0.77	0.17	0.11	1.57	46.3	21.4	32.3	0.30	0.27	0.72
26		3354–3357	AG_2^2	oil	0.56	1.01	1.13	1.03	1.22	0.25	0.15	1.65	45.0	21.5	33.5	0.23	0.25	0.71
27	Sufyan E-1	2449–2455	AG_1	oil	0.69	1.28	1.10	1.03	0.92	0.17	0.12	1.45	48.7	19.4	31.8	0.25	0.22	0.71
28	Sufyan S-1	3318–3320	AG_1	oil	0.68	1.28	1.11	1.04	0.94	0.16	0.11	1.43	46.4	21.5	32.1	0.32	0.24	0.77
29	Higra-1	3000–3003	AG_2^2	oil	0.70	1.12	1.18	1.06	1.00	0.13	0.08	1.66	42.8	24.6	32.6	0.31	0.25	0.63
30		3085–3090	AG_2^2	oil	0.66	1.09	1.18	1.07	1.04	0.16	0.10	1.78	41.5	24.1	34.4	0.28	0.21	0.62
31		2966–2968	AG_1^2	oil	0.57	0.99	1.23	1.07	1.26	0.13	0.08	1.59	39.7	24.6	35.7	0.23	0.20	0.49

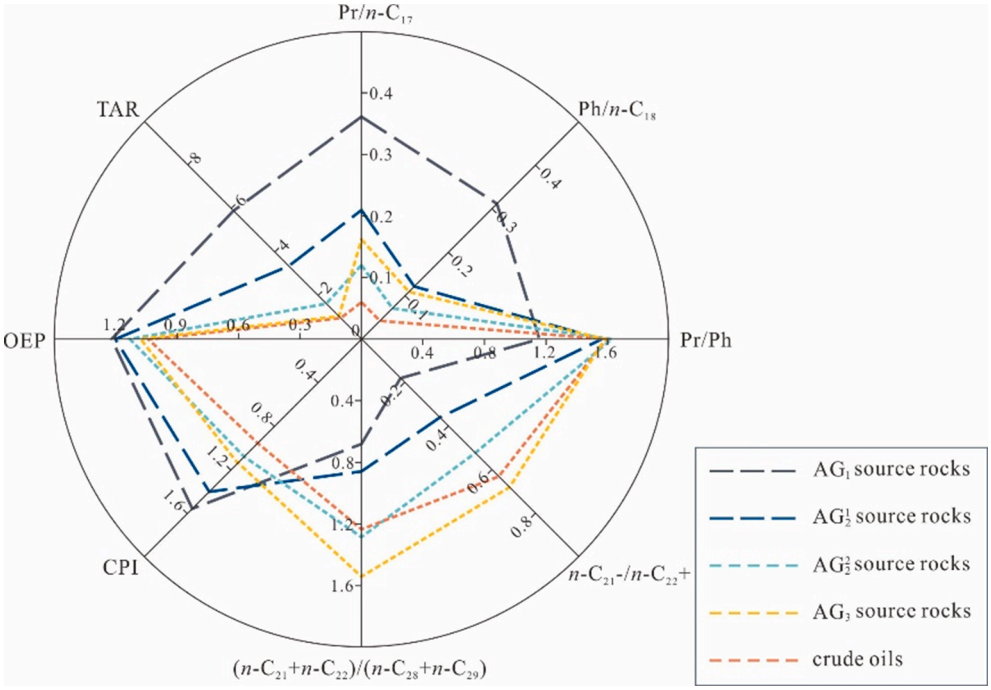

Fig. 13. Spider diagram shows the variation of average values for eight parameters in AG_1, AG_1^2, AG_2^2 and AG_3 source rocks and crude oils in the Sufyan sub-basin.

(Fig. 11), from which we infer that the water salinity of the AG_2^2 and AG_3 source rocks was higher than that of the AG_1 and AG_1^2 source rocks.

The terrigenous/aquatic ratio (TAR) is usually applied as an indicator of relative terrigenous vs aquatic organic matter input (Bourbonniere and Meyers, 1996; Xiao et al., 2019d). Relative higher TAR values in the AG_1 and AG_1^2 source rocks (>5.0) indicate more terrigenous contribution than that of the AG_2^2 and AG_3 source rocks (<3.0) (Fig. 11). The C_{27}-C_{29} regular steranes distribution indicates that the AG_1 and AG_1^2 source rocks are rich in terrigenous C_{29} steranes ($C_{27}/C_{29}St < 1.0$), while the AG_2^2 and AG_3 source rocks contain high abundance of C_{27} steranes ($C_{27}/C_{29}St > 1.0$) produced from algae and other lower aquatic organisms.

4.3. Oil-oil and oil-source rock correlations

Oil-oil and oil-source rock correlations can guide future petroleum exploration. The influence of source facies, thermal maturity, and reservoir alteration processes must be considered and the correlations become more credible using a multiple parameters approach (Peters et al., 2005). Some crude oils found in shallow reservoirs in the Muglad

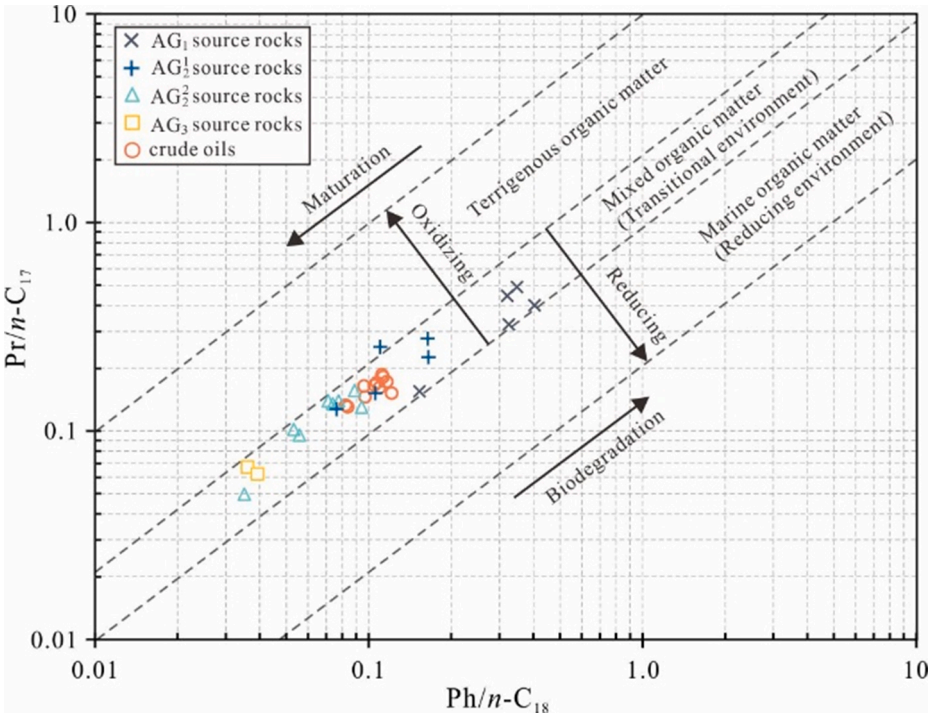

Fig. 14. Phytane to n-C_{18} (Ph/n-C_{18}) versus pristane to n-C_{17} (Pr/n-C_{17}) showing various depositional environments and organic matter type (Shanmugam, 1985).

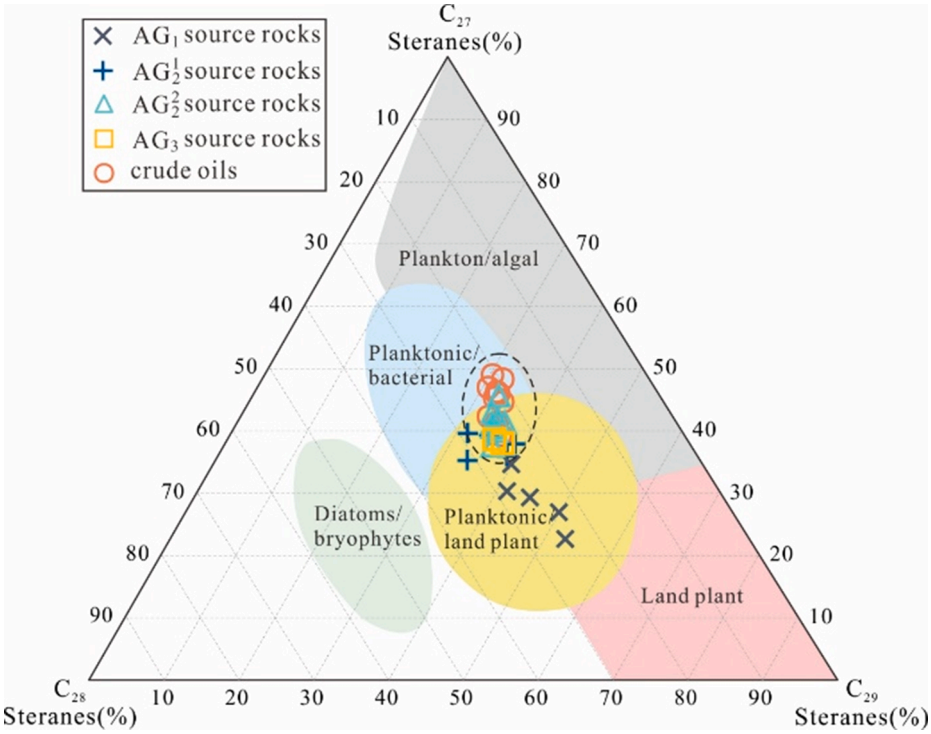

Fig. 15. Ternary diagram of C_{27}–C_{29} regular steranes showing various organic matter inputs and the relationship between source rocks and crude oils (after Huang and Meinschein, 1979).

Basin have suffered various degrees of biodegradation (Nie et al., 2004; Dou et al., 2006; Yang et al., 2019). However, all crude oils in this study possess a complete distribution of C_{12}–C_{38} *n*-alkanes (Fig. 12) and 25-norhopanes were not detected, indicating that biodegradation is absent or inconsequential and is not a factor that needs to be considered. Furthermore, there is no evidence that other reservoir alteration processes (e.g., phase separation, water/gas washing, thermal cracking, thermochemical sulfate reduction) have altered the composition of the Abu Gabra Formation oil samples. Consequently, source-, thermal maturity- and depositional condition-related parameters can provide a reliable correlation between oils and their source.

All distribution of biomarkers and geochemical properties imply that the oils produced in the Abu Gabra Formation correlate and were generated from source rocks in the AG_2^2 and AG_3 members (Table 3). No

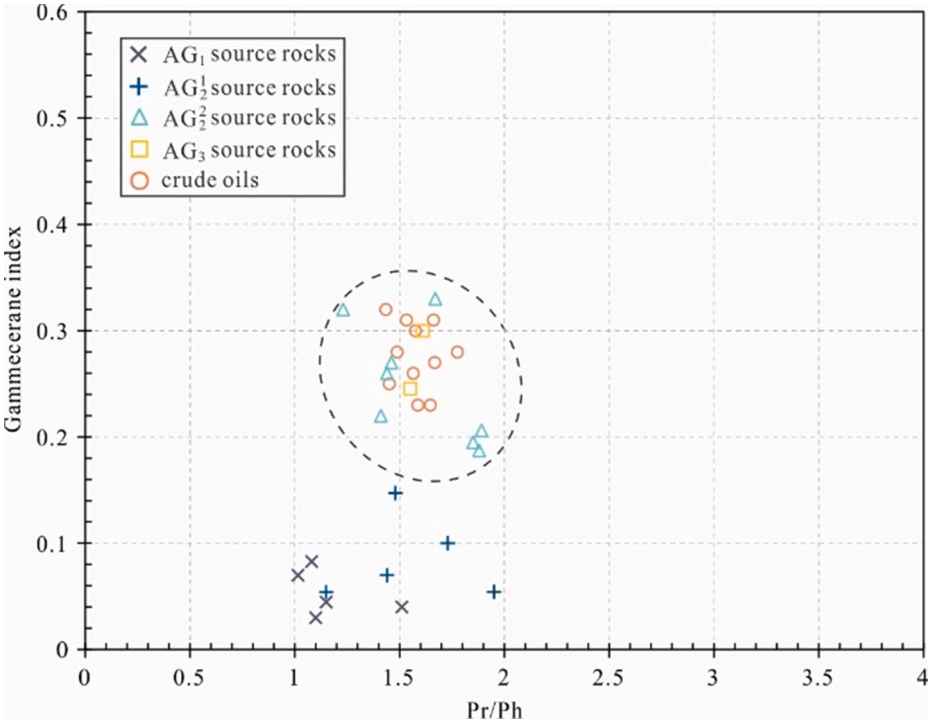

Fig. 16. Pr/Ph vs $Ga/C_{30}H$ ratios indicative of depositional conditions of organic matter.

contribution from the source facies in the AG_1 and AG_1^2 members is detectable, which strongly indicates that the lower AG_2^2 and AG_3 members are the major source of the Abu Gabra oils, including those produced from the AG_1 and AG_1^2 members. An examination of individual molecular distributions and biomarker ratios supports this conclusion.

A line chart summarizing the relative abundance of C_{14}–C_{36} *n*-alkanes show that the crude oil samples correlate well with each other. Since these distributions are influenced by both organic facies and level of thermal maturity it is not surprising that the oils correlate best with rock extracts in the lower AG_2^2 and AG_3 members, which have entered the oil window, and poorly with the upper AG_1 and AG_1^2 members, which are immature to marginally mature (Fig. 12).

This correlation between source input and thermal maturity is evident in several *n*-alkane parameters, *n*-C_{21}-/*n*-C_{21}+, (*n*-C_{21} + *n*-C_{22})/(*n*-C_{28} + *n*-C_{29}), carbon preference index (CPI), odd-to-even predominance (OEP) and the terrigenous/aquatic index (TAR) (Table 3). TAR is the ratio of (*n*-C_{27} + *n*-C_{29} + *n*-C_{31})/(*n*-C_{15} + *n*-C_{17} + *n*-C_{19}) that reflects the relative input of leaf waxes to algal derived *n*-alkanes (Bourbonniere and Meyers, 1996). A radar chart plotting the *n*-alkane and isoprenoid ratios for the average values in the AG_1, AG_1^2, AG_2^2 and AG_3 source rocks and crude oils shows the clear affinity of the deeper facies to the produced oils (Fig. 13). The AG_1 and AG_1^2 source rocks have relatively higher TAR, CPI and OEP values, and lower values of *n*-C_{21}-/*n*-C_{21} + and (*n*-C_{21} + *n*-C_{22})/(*n*-C_{28} + *n*-C_{29}) than those of the AG_2^2 and AG_3 source rocks and crude oils (Fig. 13). All crude oils correlate well with the AG_2^2 and AG_3 source rocks, and the hydrocarbon contribution from the AG_1 and AG_1^2 source rocks is limited and not detectable.

The values of Pr/Ph ratio in the crude oils range from 1.43 to 1.78 and are within the range seen in source rock extracts from all members of the Abu Graba Formation and are not diagnostic of a specific source. Ph/*n*-C_{18} vs Pr/*n*-C_{17} is a common plot that illustrates general depositional conditions and relative maturity (Shanmugam, 1985; Mashhadi and Rabbani, 2015; Lai et al., 2018). The source rock extracts and crude oils fall into the same zone for a transitional environment under generally sub-oxic depositional conditions with the AG_2^2 and AG_3 source rocks and crude oils have lower values of Ph/*n*-C_{18} and Pr/*n*-C_{17} ratios, consistent with a higher level of thermal maturity than the AG_1 and AG_1^2 samples (Fig. 14).

The AG_2^2 and AG_3 members and crude oils exhibit a similar steranes distribution pattern with a predominance of C_{27} steranes over C_{29} steranes (Fig. 15). This distribution pattern is also present in several rock extracts from the AG_1^2 member, but most of the AG_1 and AG_1^2 source rocks have a distinctly lower concentration of C_{27} steranes and higher C_{29} steranes compared to the oils and the AG_2^2 and AG_3 source rocks (Table 3). The distributions are consistent with the Abu Gabra Formation source rocks containing mixed contributions of planktonic algae, bacteria and terrigenous plant materials with the proportion of terrigenous plant materials higher in the AG_1 and AG_1^2 than the AG_2^2 and AG_3 members.

Other biomarker parameters provide confirmation of correlation between the lower Abu Graba members and produced oils. The AG_2^2 and AG_3 source rocks have relatively higher values of the Gammacerane Index (gammacerane/C_{30} 17α(H),21β(H)-hopane, 0.19–0.33) than that of the AG_1 (0.03–0.08) and AG_1^2 (0.05–0.15) source rocks, suggesting lacustrine deposition transitioned from saline to freshwater (Fig. 16). Higher gammacerane indices also are observed in the oil samples correlating with the organic facies present in the AG_2^2 and AG_3 source rocks.

Sterols are catalytically converted by clays into diasterenes during diagenesis and are ultimately reduced to diasteranes, hence the ration of diasteranes to steranes reflects source rock lithology (Peters et al., 2005). A similar process converts hopanols into diahopanes and the C_{27}Dia/C_{27}St and C_{30}D/C_{30}H ratios can be used to compare relative content of clay minerals in source rocks and related oils (Xiao et al., 2019b). These ratios also increase at higher levels of maturation due to differences in thermal stability, but this factor need not be considered in the Sufyan sub-basin samples. All crude oils from the Sufyan sub-basin contain high abundance of diasteranes and diahopanes, and the values of C_{27}Dia/C_{27}St and C_{30}D/C_{30}H range from 0.49 to 0.88 (average 0.71) and 0.20 to 0.37 (average 0.26) (Fig. 17), respectively. The AG_2^2 and AG_3 source rocks show a similar distribution of diasteranes (C_{27}Dia/C_{27}St = 0.71) and diahopanes (C_{30}D/C_{30}H = 0.24) to crude oils, consistent with a clay-rich and oxic to sub-oxic depositional environments. The AG_1 and AG_1^2 source rocks have relatively low content of diasteranes (C_{27}Dia/C_{27}St = 0.40) and diahopanes (C_{30}D/C_{30}H = 0.06) corresponding to a clay-poor and immature source rock (Fig. 17).

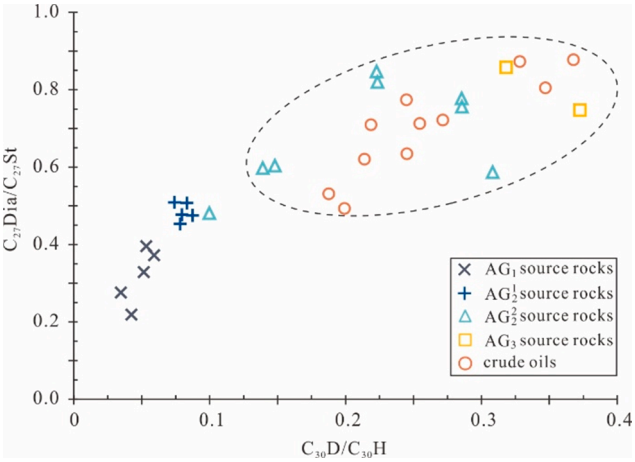

Fig. 17. The distributions of diahopanes and diasteranes in crude oils and source rocks reflecting the variation of depositional conditions.

5. Conclusions

The molecular characteristics of the Cretaceous Aba Gabra Formation rock and oil samples were characterized in order to reveal the heterogeneity in organic facies from different members and submembers and to determine their relative hydrocarbon contribution to discovered crude oils. Not all mudstone members of the Abu Gabra Formation are effective source rocks. The selection of only high TOC samples will exaggerate the petroleum resource potential of a unit. Broader sampling is needed to determine the influence of geochemical heterogeneity that occurs within thick source rock intervals.

A total of 228 rock cuttings were collected for Rock-Eval pyrolysis and TOC analyses and twenty source rocks and eleven crude oils were systematically analyzed for biomarker compositions. Detailed geochemical assessment of rock cuttings presents an obvious vertical geochemical heterogeneity within the Abu Gabra Formation. The lower AG_2^2 and AG_3 source rocks have better quality (e.g., kerogen type, % TOC and maturity) than the upper AG_1^2 and AG_1 source rocks, which is mainly controlled by the biological composition, burial depth, and depositional conditions for organic matter preservation. Biomarker investigation of rock extracts and crude oils shows that all studied oils have a close genetic relationship indicating a single oil family that is mostly derived from the AG_2^2 and AG_3 source rocks with limited contribution from AG_1 and AG_1^2 source rocks.

Declaration of Competing Interest

The authors declare that they have no known competing financial interests or personal relationships that could have appeared to influence the work reported in this paper.

Acknowledgments

The authors would like to thank Dr. John K. Volkman (Co-Editor-in-Chief), two anonymous reviewers, and especially Dr. Clifford Walters (Associate Editor) for their constructive comments and suggestions which significantly improved the quality of the manuscript. This work was supported by the Science Foundation of China University of Petroleum, Beijing (No. 2462021XKBH001) and the National Key Project (No. 2016ZX05029). We are grateful for laboratory assistance by Lei Zhu, Shengbao Shi and Jianfeng Zhang. We would like to thank the Research Institute of Petroleum Exploration and Development, PetroChina for providing samples, and for permission to publish this work.

References

Aquino Neto, F.R., Trendel, J.M., Restlé, A., Connan, J., Albrecht, P., 1983. Occurrence and formation of tricyclic terpanes in sediments and petroleums. In: Bjorøy, M., Albrecht, P., Cornford, C., de Groot, K., Eglinton, G., Galimov, E., Leythaeuser, D., Pelet, R., Rullkötter, J., Speers, G. (Eds.), Advances in Organic Geochemistry 1981. Wiley, Chichester, pp. 659–667.

Banta, A.B., Wei, J.H., Welander, P.V., 2015. A distinct pathway for tetrahymanol synthesis in bacteria. Proceedings of the National Academy of Sciences 112, 13478–13483.

Bourbonniere, R.A., Meyers, P.A., 1996. Sedimentary geolipid records of historical changes in the watersheds and productivities of Lakes Ontario and Erie. Limnology and Oceanography 41, 352–359.

Bray, E.E., Evans, E.D., 1961. Distribution of *n*-paraffins as a clue to recognition of source beds. Geochimica et Cosmochimica Acta 22, 2–15.

Chen, Z., Liu, G., Wei, Y., Gao, G., Ma, W., 2017. Distribution pattern of tricyclic terpanes and its influencing factors in the Permian source rocks from Mahu Depression in the Junggar Basin. Oil and Gas Geology 38, 311–322 (in Chinese with English abstract).

Dou, L., Cheng, D., Zhi, L., Zhang, Z., Wang, J., 2013. Petroleum geology of the Fula Sub-basin, Muglad Basin, Sudan. Journal of Petroleum Geology 36, 43–59.

Dou, L., Zhang, Z., Cheng, D., 2006. Regional seal control on oil accumulation in Muglad Basin of Sudan. Acta Petrolei Sinica 27, 22–26 (in Chinese with English abstract).

Ekweozor, C., Strausz, O., 1983. Tricyclic terpanes in the Athabasca oil sands: Their geochemistry. In: Bjorøy, M., Albrecht, P., Cornford, C., de Groot, K., Eglinton, G., Galimov, E., Leythaeuser, D., Pelet, R., Rullkötter, J., Speers, G. (Eds.), Advances in Organic Geochemistry 1981. Wiley, Chichester, pp. 746–766.

Fairhead, J.D., 1988. Mesozoic plate tectonic reconstructions of the central South Atlantic Ocean: The role of the West and Central African rift system. Tectonophysics 155, 181–191.

Fu, J., Zhang, Z., Chen, C., Wang, T.G., Li, M., Ali, S., Lu, X., Dai, J., 2019. Geochemistry and origins of petroleum in the Neogene reservoirs of the Baiyun Sag, Pearl River Mouth Basin. Marine and Petroleum Geology 107, 127–141.

Genik, G.J., 1993. Petroleum geology of rift basins in Niger, Chad, and Central African Republic. American Association of Petroleum Geologists Bulletin 77, 1405–1434.

Hao, F., Zhou, X., Zhu, Y., Yang, Y., 2011. Lacustrine source rock deposition in response to co-evolution of environments and organisms controlled by tectonic subsidence and climate, Bohai Bay Basin, China. Organic Geochemistry 42, 323–339.

Hao, F., Zou, H., Gong, Z., Deng, Y., 2007. Petroleum migration and accumulation in the Bozhong sub-basin, Bohai Bay Basin, China: significance of preferential petroleum migration pathways (PPMP) for the formation of large oilfields in lacustrine fault basins. Marine and Petroleum Geology 24, 1–13.

Hills, I.R., Whitehead, E.V., Anders, D.E., Cummins, J.J., Robinson, W.E., 1966. An optically active triterpane, gammacerane in Green River, Colorado, oil shale bitumen. Chemical Communications 20, 752–754.

Huang, W.Y., Meinschein, W.G., 1979. Sterols as ecological indicators. Geochimica et Cosmochimica Acta 43, 739–745.

Hunt, J.M., 1996. Petroleum Geochemistry and Geology. Freeman.

Lai, H., Li, M., Liu, J., Mao, F., Xiao, H., He, W., Yang, L., 2018. Organic geochemical characteristics and depositional models of Upper Cretaceous marine source rocks in the Termit Basin, Niger. Palaeogeography, Palaeoclimatology, Palaeoecology 495, 292–308.

Lai, H., Li, M., Liu, J., Mao, F., Wang, Z., Liu, W., Xiao, H., Yang, L., 2019. Source rock assessment within a sequence stratigraphic framework of the Yogou Formation in the Termit Basin, Niger. Geological Journal 55, 2473–2494.

Liu, Q., Song, Y., Jiang, L., Cao, T., Chen, Z., Xiao, D., Han, G., Ji, W., Gao, F., Wang, P., 2017. Geochemistry and correlation of oils and source rocks in Banqiao Sag, Huanghua Depression, northern China. International Journal of Coal Geology 176–177, 49–68.

Luo, X., Shan, X., Zhang, T., Xu, S., 1998. Discussion on the characteristics of organic macerals and the hydrocarbon generating potential of the source rock in M Basin. Journal of Xi'an Petroleum Institute 13, 28–30 (in Chinese with English abstract).

Mackenzie, A.S., Brassell, S.C., Eglinton, G., Maxwell, J.R., 1982. Chemical fossils: the geological fate of steroids. Science 217, 491–504.

Makeen, Y.M., Wan, H.A., Hakimi, M.H., Elhassan, O.M.A., 2015a. Organic geochemical characteristics of the Lower Cretaceous Abu Gabra Formation in the Great Moga oilfield, Muglad Basin, Sudan: implications for depositional environment and oil-generation potential. Journal of African Earth Sciences 103, 102–112.

Makeen, Y.M., Wan, H.A., Hakimi, M.H., Mustapha, K.A., 2015b. Source rock characteristics of the Lower Cretaceous Abu Gabra Formation in the Muglad Basin, Sudan, and its relevance to oil generation studies. Marine and Petroleum Geology 59, 505–516.

Mashhadi, Z.S., Rabbani, A.R., 2015. Organic geochemistry of crude oils and Cretaceous source rocks in the Iranian sector of the Persian Gulf: An oil-oil and oil-source rock correlation study. International Journal of Coal Geology 146, 118–144.

McHargue, T.R., Heidrick, T.L., Livingston, J.E., 1992. Tectonostratigraphic development of the Interior Sudan rifts, Central Africa. Tectonophysics 213, 187–202.

Mohamed, A.Y., Pearson, M.J., Ashcroft, W.A., Whiteman, A.J., 2002. Petroleum maturation modelling, Abu Gabra-Sharaf area, Muglad Basin, Sudan. Journal of African Earth Sciences 35, 331–344.

Moldowan, J.M., Seifert, W.K., Gallegos, E.J., 1985. Relationship between petroleum composition and depositional environment of petroleum source rock. American Association of Petroleum Geologists Bulletin 69, 1255–1268.

Moldowan, J.M., Fago, F.J., Carlson, R.M.K., Young, D.C., van Duyne, G., Clardy, J., Schoell, M., Pillinger, C.T., Watt, D.S., 1991. Rearranged hopanes in sediments and petroleum. Geochimica et Cosmochimica Acta 55, 3333–3353.

Mukhopadhyay, P.K., Wade, J.A., Kruge, M.A., 1995. Organic facies and maturation of Jurassic/Cretaceous rocks, and possible oil-source rock correlation based on pyrolysis of asphaltenes, Scotia Basin, Canada. Organic Geochemistry 22, 85–104.

Nie, C., Chen, F., Bai, Y., Wang, W., Ma, P., 2004. Geological characteristics of Fula oilfield in Muglad basin, Sudan. Oil and Gas Geology 25, 671–676 (in Chinese with English abstract).

Peters, K.E., Moldowan, J.M., 1991. Effects of source, thermal maturity, and biodegradation on the distribution and isomerization of homohopanes in petroleum. Organic Geochemistry 17, 47–61.

Peters, K.E., Walters, C.C., Moldowan, J.M., 2005. The Biomarker Guide: Biomarkers and Isotopes in Petroleum Exploration and Earth History. Second Ed. vol 2. Cambridge University Press, Cambridge.

Qiao, J., Liu, L., An, F., Xiao, F., Wang, Y., Wu, K., Zhao, Y., 2016. Hydrocarbon potential evaluation of the source rocks from the Abu Gabra Formation in the Sufyan Sag, Muglad Basin, Sudan. Journal of Africa Earth Sciences 118, 301–312.

Scalan, E.S., Smith, J.E., 1970. An improved measure of the odd-even predominance in the normal alkanes of sediment extracts and petroleum. Geochimica et Cosmochimica Acta 34, 611–620.

Schull, T.J., 1988. Rift basins of interior Sudan: petroleum exploration and discovery. American Association of Petroleum Geologists Bulletin 72, 1128–1142.

Seifert, W., Moldowan, J., 1986. Use of biological markers in petroleum exploration. Methods in Geochemistry and Geophysics 24, 261–290.

Seifert, W.K., Moldowan, J.M., 1981. Paleoreconstruction by biological markers. Geochimica et Cosmochimica Acta 45, 783–794.

Shanmugam, G., 1985. Significance of coniferous rain forests and related organic matter in generating commercial quantities of oil, Gippsland Basin. American Association of Petroleum Geologists Bulletin 69, 1241–1254.

Sinninghe Damsté, J.S., Kenig, F., Koopmans, M.P., Köster, J., Schouten, S., Hayes, J.M., de Leeuw, J.W., 1995. Evidence for gammacerane as an indicator of water column stratification. Geochimica et Cosmochimica Acta 59, 1895–1900.

Summons, R.E., Douglas, H.E., 2018. Chemical clues to the earliest animal fossils. Science 361, 1198–1199.

Summons, R.E., Volkman, J.K., Boreham, C.J., 1987. Dinosterane and other steroidal hydrocarbons of dinoflagellate origin in sediments and petroleum. Geochimica et Cosmochimica Acta 51, 3075–3082.

Summons, R.E., Thomas, J., Maxwell, J.R., Boreham, C.J., 1992. Secular and environmental constraints on the occurrence of dinosterane in sediments. Geochimica et Cosmochimica Acta 56, 2437–2444.

Venkatesan, M.I., Dahl, J., 1989. Organic geochemical evidence for global fires at the Cretaceous/Tertiary boundary. Nature 338, 57–60.

Wang, Y., Liu, L., An, F., Wang, H., Pang, X., 2016. Maturation history modeling of Sufyan Depression, northwest Muglad Basin, Sudan. Journal of African Earth Sciences 120, 70–76.

Wen, Z., Tang, Y., Yu, Q., 2007. Crude oil geochemical characteristics of Block 6 in Sudan Muglad Basin. Journal of Oil & Gas Technology 29, 66–70 (in Chinese with English abstract).

Wu, D., Zhu, X., Zhi, L.I., Su, Y.D., Liu, Y., Zhang, M., Song, J., Liu, A., Chen, X., Zhao, D., 2015. Depositional models in Cretaceous rift stage of Fula sag, Muglad Basin, Sudan. Petroleum Exploration and Development 42, 348–357.

Xiao, H., Wang, T.-G., Li, M., Fu, J., Tang, Y., Shi, S., Yang, Z., Lu, X., 2018. Occurrence and distribution of unusual tri- and tetracyclic terpanes and their geochemical significance in some Paleogene oils from China. Energy & Fuels 32, 7393–7403.

Xiao, H., Li, M., Liu, J., Mao, F., Cheng, D., Yang, Z., 2019a. Oil-oil and oil-source rock correlations in the Muglad Basin, Sudan and South Sudan: New insights from molecular markers analyses. Marine and Petroleum Geology 103, 351–365.

Xiao, H., Li, M., Wang, W., You, B., Liu, X., Yang, Z., Liu, J., Chen, Q., Uwiringiyimana, M., 2019b. Identification, distribution and geochemical significance of four rearranged hopane series in crude oil. Organic Geochemistry 138, 103929.

Xiao, H., Li, M., Yang, Z., Zhu, Z., 2019c. The distribution patterns and geochemical implication of C_{19}–C_{23} tricyclic terpanes in source rocks and crude oils occurred in various depositional environment. Acta Geochemica 48, 161–170 (in Chinese with English abstract).

Xiao, H., Wang, T.G., Li, M., Lai, H., Liu, J., Mao, F., Tang, Y., 2019d. Geochemical characteristics of Cretaceous Yogou Formation source rocks and oil-source correlation within a sequence stratigraphic framework in the Termit Basin, Niger. Journal of Petroleum Science and Engineering 172, 360–372.

Xu, J., Luo, X., Wang, H., 2003. Source rock evaluation and crude oil geochemistry in the Fula Depression, M-Basin, East Africa. Petroleum Exploration and Development 30, 122–126 (in Chinese with English abstract).

Yang, Z., Li, M., Cheng, D., Xiao, H., Lai, H., Chen, Q., 2019. Geochemistry and possible origins of biodegraded oils in the Cretaceous reservoir of the Muglad Basin and their application in hydrocarbon exploration. Journal of Petroleum Science and Engineering 173, 889–898.

Yassin, M.A., Hariri, M.M., Abdullatif, O.M., Korvin, G., Makkawi, M., 2017. Evolution history of transtensional pull-apart, oblique rift basin and its implication on hydrocarbon exploration: a case study from Sufyan Sub-basin, Muglad Basin, Sudan. Marine and Petroleum Geology 79, 282–299.

Yassin, M.A., Hariri, M.M., Abdullatif, O.M., Makkawi, M., Bertotti, G., Kaminski, M.A., 2018. Sedimentologic and reservoir characteristics under a tectono-sequence stratigraphic framework: A case study from the Early Cretaceous, upper Abu Gabra sandstones, Sufyan Sub-basin, Muglad Basin, Sudan. Journal of African Earth Sciences 142, 22–43.

Zhang, Y., 2007. Petroleum system in the Sufyan Depression of Muglad Basin in Sudan. Petrol. Geol. Exp. 29, 572–576 (in Chinese with English abstract).

Zhang, Y., Qin, G.U., 2009. Petroleum system of the Sufyan Depression at the eastern margin of a huge strike-slip fault zone in Central Africa. Acta Geologica Sinica (English Edition) 83, 1182–1187.

Zhao, Y.J., Han, Y.C., Liu, X.N., Yong-Jun, Y.U., Wang, J.C., 2008. Petroleum geologic feature and exploration potential of Sufyan Depression, Muglad Basin. Journal of Oil & Gas Technology 30, 19–23 (in Chinese with English abstract).

Zhu, D., Jin, Z., 2008. Effects of abnormally high heat stress on petroleum in reservoir—An example from the Tazhong 18 Well in the Tarim Basin. Science China Series D 51, 515–527 (in Chinese with English abstract).

Zhu, Y., 1997. Geochemical characteristics of terrestrial oils of the Tarim Basin. Acta Sedimentologica Sinica 15, 26–30 (in Chinese with English abstract).